Journal of Electrical Engineering, Vol. 75, No. 1, 2024, pp. 63-71

sciendo
PAPERS

A simple design of low-loss quad-band Wilkinson power dividers

Nguyen Minh Giang*, Le Ho Manh Thang, Le Dang Manh, Tran Thi Thu Huong

In this paper, a novel design method for quad-band Wilkinson power dividers is proposed. The design method is based on using a quad-band microstrip line. In comparison with other design methods, the proposed method has the advantages of simplicity and low insertion loss. To validate the proposed method, an equal quad-band power divider operating at four bands of 0.7, 1.2, 1.78, and 2.28 GHz was simulated and measured. Good agreement between measured results and simulated ones is obtained. The measured results show that the developed quad-band power divider features low insertion loss of less than 0.75 dB, isolation greater than 20.92 dB, and return loss better than 18 dB at four operating bands.

Keywords: Wilkinson power divider, low-loss, multiband, quad-band, microstrip coupler

1 Introduction

The power divider (PD) is an important component in communication systems. Various types of power dividers with improved features have been proposed [1-8]. Among them, multi-band PDs are attracting more and more attention. In work [9], a compact dual-band PD was designed using a π-shaped structure. In that PD, each quarter-wavelength transmission line was replaced by a dual-band equivalent π-shaped structure. Thanks to this, the circuit was capable of working on 2 bands. In [10,11], a dual-band PD was fabricated by employing a T-shaped structure. The authors in [12] used metamaterial structure to design tri-band PD with high isolation and good return losses. Up to now, there have been a few publications on quad-band power dividers. In work [13], a quad-band power divider was designed by using particle swarm optimization to calculate characteristic impedances and electrical lengths of transmission lines in the scheme. The disadvantages of this method include the use of an approximate method based on a complex optimization algorithm, and the scheme requires up to four isolation resistors, which exacerbate parasitic effects at high frequencies. In work [14,15], quad-band power dividers combined with filtering features were proposed. In [16], a quad-band power divider based on SIW technology was presented. However, the circuit in [16] has drawbacks of high loss and poor isolation. A fully planar quad-band PD based on an extended composite right and left-handed transmission line (E-CRLH-TL) was designed in [17]. The divider presented in [17] also has the disadvantage of high insertion loss. In literature, it is found that most of the reported design methods for quad-band power dividers are only applied to the design of equal quad-band power dividers and have losses above 1 dB.

In this paper, we propose a simple method to design equal quad-band Wilkinson PDs with low loss. In addition, we have verified through theory and simulation that the proposed method can be extended to design unequal quad-band Wilkinson PDs. The proposed method is based on a quad-band microstrip line. The circuit can be designed by closed-form equations. The design equations given in the paper provide a convenient way to design the equal and unequal quad-band power PDs. To evaluate the effectiveness of the design method, a quad-band power divider was designed, manufactured, and tested. The good agreement between the simulation and measurement results validated the feasibility of the proposed design method.

2 Theory and design equations of equal quad-band PDs

The traditional Wilkinson power divider circuit is shown in Fig. 1 [18]. The circuit consists of one input port (Port 1) and two output ports (Port 2 and Port 3) with characteristic impedance Z_0 of 50 Ω. In the circuit, the input line is separated into two branches with characteristic impedances Z_1 and Z_2. Each of them is the quarter-wavelength microstrip line. The resistor R_S connected between two branches to increase the isolation between the output ports.

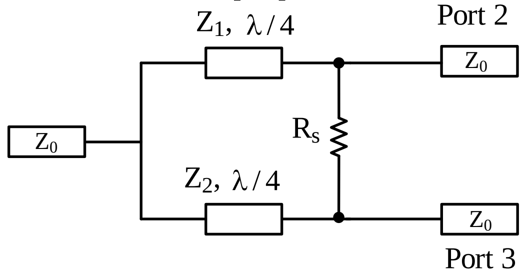

Fig. 1. Conventional equal Wilkinson power divider

Le Quy Don Technical University, 236 Hoang Quoc Viet, Ha Noi, Viet Nam
* giangnm@lqdtu.edu.vn

https://doi.org/10.2478/jee-2024-0009, Print (till 2015) ISSN 1335-3632, On-line ISSN 1339-309X

The values of impedances Z_1 and Z_2 are calculated below.

$$Z_1 = Z_2 = \sqrt{2}Z_0 \approx 70.71\,\Omega \tag{1}$$

$$R_S = 2Z_0 = 100\,\Omega \tag{2}$$

To make the power divider in Fig. 1 work at four bands, the transmission lines Z_1 and Z_2 need to be replaced by equivalent quad-band microstrip lines. Figure 2 shows a model of the quad-band microstrip line [19]. A transmission line with characteristic impedance Z_C and electrical length $\lambda/4$ is deformed to be equivalent to a quad-band microstrip line. The quad-band microstrip line is composed of a π-shaped structure and two coupled lines. The π-shaped structure consists of a series transmission line having characteristic impedance Z_A and electrical length 2θ and two short-circuited shunt stubs having characteristic impedance Z_B and electrical length θ. Two coupled lines have the same parameters of even- and odd-characteristic impedance (Z_e and Z_o) and electrical length θ.

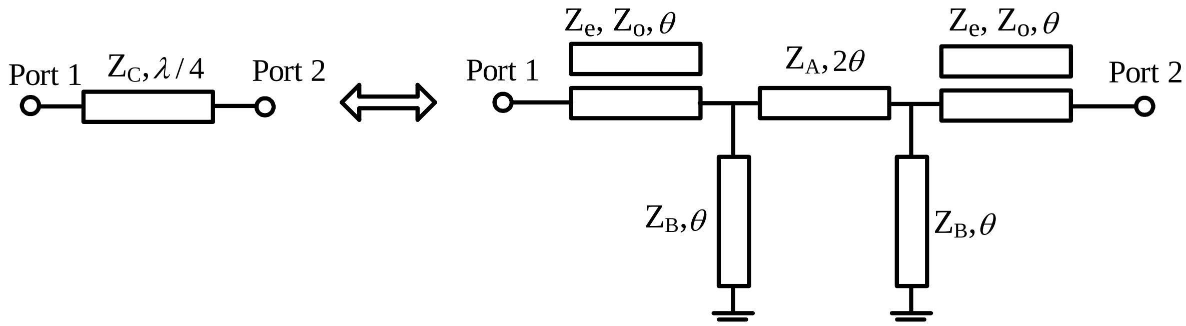

Fig. 2. A quarter-wavelength transmission line with characteristic impedance Z_C and its equivalent quad-band microstrip circuit

Matrix ABCD of the quad-band microstrip line is determined by the product of ABCD matrix of each section as follows.

$$\boldsymbol{M}_1 = \begin{bmatrix} A & B \\ C & D \end{bmatrix} = \begin{bmatrix} A_K & B_K \\ C_K & D_K \end{bmatrix}\begin{bmatrix} A_B & B_B \\ C_B & D_B \end{bmatrix}\begin{bmatrix} A_A & B_A \\ C_A & D_A \end{bmatrix}\begin{bmatrix} A_B & B_B \\ C_B & D_B \end{bmatrix}\begin{bmatrix} A_K & B_K \\ C_K & D_K \end{bmatrix} \tag{3}$$

Here,

$$\begin{bmatrix} A_K & B_K \\ C_K & D_K \end{bmatrix} = \begin{bmatrix} \cos\theta & j\dfrac{(Z_e + Z_o)\sin\theta}{2} \\ j\dfrac{2\sin\theta}{Z_e + Z_o} & \cos\theta \end{bmatrix},$$

$$\begin{bmatrix} A_B & B_B \\ C_B & D_B \end{bmatrix} = \begin{bmatrix} 1 & 0 \\ -j\frac{\cot\theta}{Z_B} & 1 \end{bmatrix},$$

$$\begin{bmatrix} A_A & B_A \\ C_A & D_A \end{bmatrix} = \begin{bmatrix} \cos2\theta & jZ_A\sin2\theta \\ j\dfrac{\sin2\theta}{Z_A} & \cos2\theta \end{bmatrix}.$$

The ABCD matrix of transmission line with characteristic impedance Z_C and electrical length $\lambda/4$ is defined below.

$$\boldsymbol{M}_2 = \begin{bmatrix} 0 & jZ_C \\ \dfrac{j}{Z_C} & 0 \end{bmatrix} \tag{4}$$

Conditions for quad-band microstrip line to be equivalent to the quarter-wavelength transmission line Z_C are determined as follows. By equalizing the elements of two matrices $\boldsymbol{M}_1$ and $\boldsymbol{M}_2$, the following equations are obtained.

$$\tan\theta = \pm\frac{2Z_C}{Z_K}\left(\sqrt{1 + \frac{(Z_K^2+4Z_C^2)^2}{64Z_C^4}} \pm \frac{Z_K^2+4Z_C^2}{8Z_C^2}\right) \tag{5}$$

$$Z_A = Z_K\left(\frac{Z_K^2 + 4Z_C^2}{16Z_C^2}\right) \tag{6}$$

$$Z_B = \frac{Z_K^3}{8Z_C^2}\left(\frac{Z_K^2 + 4Z_C^2}{4Z_C^2 - Z_K^2}\right) \tag{7}$$

Here, $Z_K = Z_e + Z_o$.

It is assumed that two circuits are equivalent at four bands f_1, f_2, f_3, f_4 $(f_1 < f_2 < f_3 < f_4)$ and corresponding electrical lengths θ_1, θ_2, θ_3, and θ_4. Then, the electrical lengths must satisfy the following conditions.

$$\theta_1 = tan^{-1}\left[\frac{2Z_C}{Z_K}\left(\sqrt{1+\frac{(Z_K^2+4Z_C^2)^2}{64Z_C^4}}-\frac{Z_K^2+4Z_C^2}{8Z_C^2}\right)\right] \quad (8)$$

$$\theta_2 = tan^{-1}\left[\frac{2Z_C}{Z_K}\left(\sqrt{1+\frac{(Z_K^2+4Z_C^2)^2}{64Z_C^4}}+\frac{Z_K^2+4Z_C^2}{8Z_C^2}\right)\right] \quad (9)$$

$$\theta_3 = \pi - \theta_2 \quad (10)$$

$$\theta_4 = \pi - \theta_1 \quad (11)$$

The following relations between four operating frequencies are obtained:

$$f_2 = f_1\frac{\theta_2}{\theta_1},\ f_3 = f_2\left[\frac{\pi}{\theta_2}-1\right],\ f_4 = f_1\left[\frac{\pi}{\theta_1}-1\right] \quad (12)$$

A quad-band power divider is obtained by replacing quarter-wavelength transmission lines Z_1 and Z_2 of the conventional Wilkinson PD in Fig. 1 with quad-band microstrip lines. The proposed quad-band PD is presented in Fig. 3.

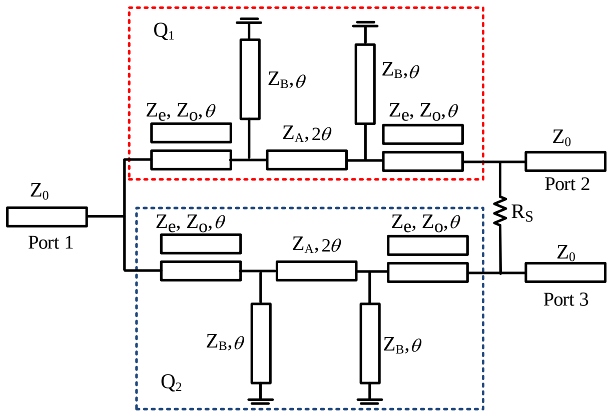

Fig. 3. The proposed structure of equal quad-band PD

Design parameters of the equal quad-band PD are calculated by using Eqns. (5-12). The design procedure of the equal quad-band PD is summarized as follows:

1. Select the operating frequencies f_1, f_4
2. From (12), define electrical length θ_1
3. From (8), set Z_C=70.71 Ω and calculate impedance Z_K
4. From (9), define electrical length θ_2
5. Determine frequencies f_2 and f_3 from (12)
6. Calculate Z_A and Z_B by Eqns (6) and (7)

In the next part, we will study the design limitations of the proposed equal quad-band PD. The circuit can be fabricated by normal PCB technology if characteristic impedances Z_A and Z_B of the scheme have values between 15 Ω and 120 Ω. The reason is that if the impedance of a transmission line is too high, the width of the line will be too narrow and difficult to manufacture. Vice versa, if the impedance is too low, the width of the transmission line will be too large and the loss will be high. Set $n_1 = f_4/f_1$ and $n_2 = f_3/f_2$. Based on Eqns. (6-12), the dependences of impedances Z_A and Z_B versus the coefficients n_1 and n_2 are illustrated in Fig. 4. As observed from Fig. 4, to keep the impedances Z_A and Z_B in the range from 15 Ω to 120 Ω, operating frequencies of the proposed quad-band PD must satisfy the following conditions:

$$2.75 \le \frac{f_4}{f_1} \le 4.5, \qquad 1.44 \le \frac{f_3}{f_2} \le 1.58. \quad (13)$$

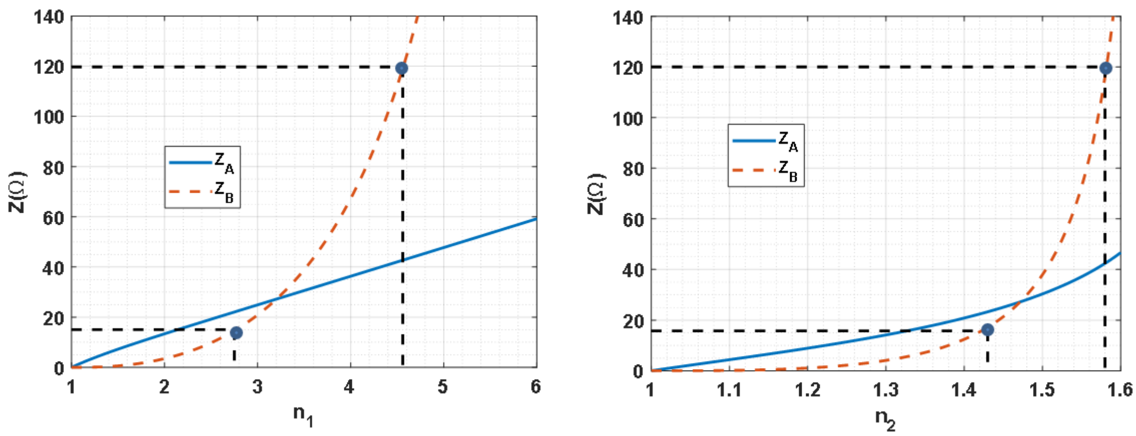

Fig. 4. (a) Dependence of characteristic impedances Z_A and Z_B versus coefficients n_1.
(b) Dependence of characteristic impedances Z_A and Z_B versus coefficients n_2.

3 Theory and design equations of unequal quad-band PDs

The conventional unequal quad-band PD is presented in Fig. 5 [18]. The schematic of the unequal quad-band PD is quite similar to that of the equal quad-band PD (Fig. 1). The differences are that characteristic impedances of the output ports Z_a and Z_b are different from Z_0, and the value of isolation resistor R_a is calculated according to power split ratio. Two branches have characteristic impedances Z_{a1} and Z_{a2}. We denote P_1, P_2 and P_3 the powers at ports 1, 2, and 3, respectively. The power split ratio between port 2 and port 3 is $K^2 = \frac{P_3}{P_2}$.

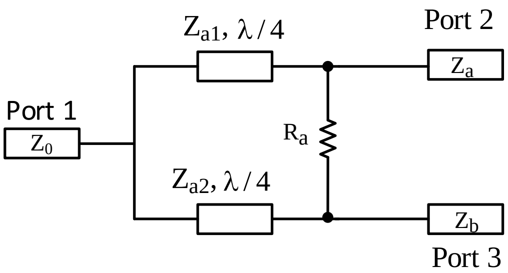

Fig. 5. Schematic of the conventional unequal quad-band PD

According to [18], the following equations are obtained:

$$Z_{a1} = Z_0\sqrt{K(1+K^2)} \tag{14}$$

$$Z_{a2} = Z_0\sqrt{\frac{1+K^2}{K^3}} \tag{15}$$

$$Z_a = Z_0 K \tag{16}$$

$$Z_b = \frac{Z_0}{K} \tag{17}$$

$$R_a = Z_0\left(K + \frac{1}{K}\right) \tag{18}$$

Since output impedances Z_a and Z_b are different from standard impedance Z_0 (50 Ω), these impedances need to be converted to Z_0. The modified unequal quad-band PD is presented in Fig. 6.

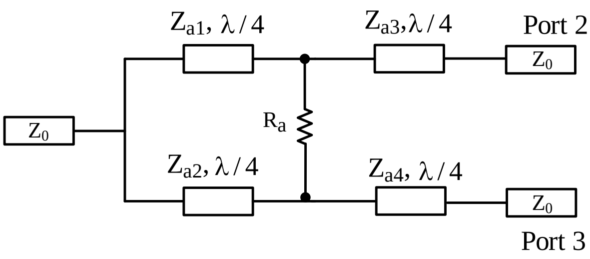

Fig. 6. Modified unequal Wilkinson PD

Impedances Z_{a3} and Z_{a4} are determined by the following expressions.

$$Z_{a3} = \sqrt{Z_0 \cdot Z_a} = Z_0\sqrt{K} \tag{19}$$

$$Z_{a4} = \sqrt{Z_0 \cdot Z_b} = \frac{Z_0}{\sqrt{K}} \tag{20}$$

To make the power divider work at four bands, the transmission lines Z_{a1}, Z_{a2}, Z_{a3}, and Z_{a4} are replaced with quad-band microstrip lines (blocks) Q_1, Q_2, Q_3, and Q_4, respectively. Then, the proposed unequal quad-band PD is presented in Fig. 7.

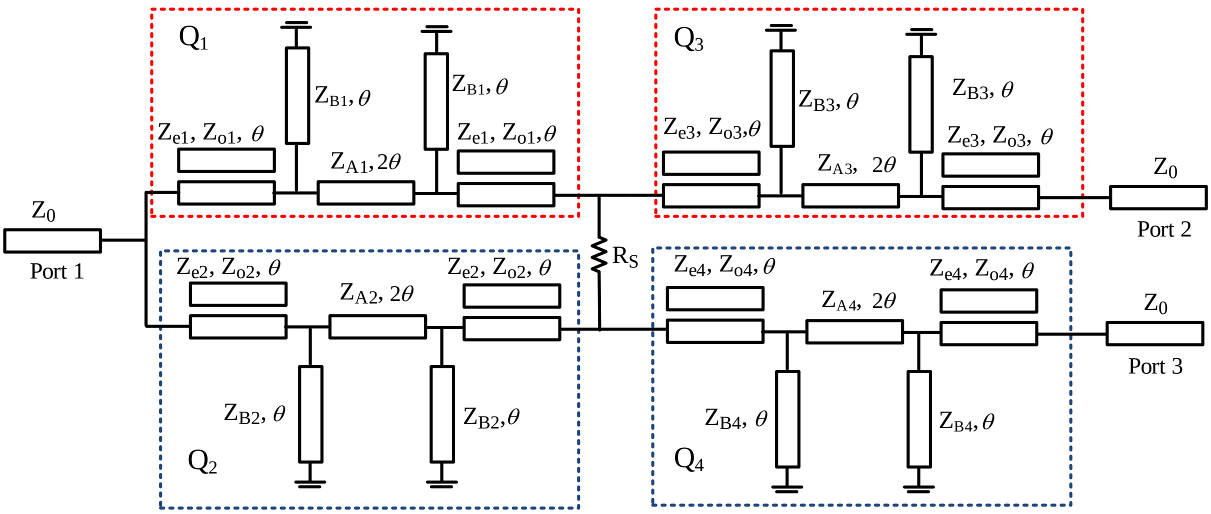

Fig. 7. Schematic of the proposed unequal quad-band PD

The design parameters of 4 blocks Q_1, Q_2, Q_3, and Q_4 can be determined by using the design procedure of the equal quad-band PD in Section 2. In this case, it should be noted that the value Z_C in step 3 of the design procedure for blocks Q_1, Q_2, Q_3, and Q_4 will receive the values Z_{a1}, Z_{a2}, Z_{a3}, and Z_{a4}, respectively.

For demonstration, an unequal quad-band PD with a power split ratio $K^2 = P_3/P_2 = 1.5$ and four operating bands of 0.9, 1.68, 2.55, and 3.33 GHz is designed. Applying Eqns. (14-20), impedances of the PD circuit in Fig. 6 are calculated as $Z_{a1} = 87.49\ \Omega$, $Z_{a2} = 58.33\ \Omega$, $Z_{a3} = 55.33\ \Omega$, $Z_{a4} = 45.18\ \Omega$, $R_a = 102\ \Omega$. Then, the design parameters of 4 blocks Q_1, Q_2, Q_3, and Q_4 are determined as follows.

- For block Q_1: $Z_C = Z_{a1} = 87.49\ \Omega$, $Z_{K1} = 114.15\ \Omega$, $Z_{A1} = 40.68\ \Omega$, $Z_{B1} = 60.28\ \Omega$, $\theta = 38.3^0\ \Omega$
- For block Q_2: $Z_C = Z_{a2} = 58.33\ \Omega$, $Z_{K2} = 76.11\ \Omega$, $Z_{A2} = 27.13\ \Omega$, $Z_{B2} = 40.2\ \Omega$
- For block Q_3: $Z_C = Z_{a3} = 55.33\ \Omega$, $Z_{K3} = 72.19\ \Omega$, $Z_{A3} = 25.73\ \Omega$, $Z_{B3} = 38.12\ \Omega$
- For block Q_4: $Z_C = Z_{a4} = 45.18\ \Omega$, $Z_{K4} = 58.94\ \Omega$, $Z_{A4} = 21.01\ \Omega$, $Z_{B4} = 31.11\ \Omega$.

Based on the above calculation results, the unequal quad-band PD is simulated using Keysight ADS software. The ideal simulated S-parameters of the unequal quad-band PD are presented in Fig. 8.

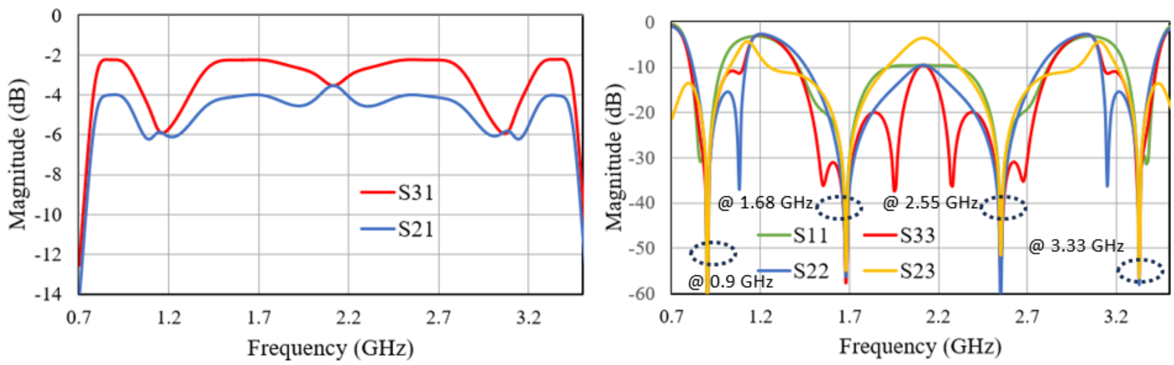

Fig. 8. Ideal simulated S-parameters of the unequal quad-band PD with power split ratio K^2= 1.5, and operating frequencies 0.9, 1.68, 2.55 and 3.33 GHz

From Fig. 8, it is clear that insertion losses of ports 3 and 2 at four bands have values of 2.2 ± 0.01 dB and 3.98 ± 0.02 dB, respectively. Therefore, the simulation results are consistent with the theory with errors below 0.02 dB. Other scattering parameters including S_{11}, S_{22}, S_{33}, and S_{23} are better than 40 dB at four operating bands. These simulation results verify the accuracy of the proposed design method.

Next, the fabrication limitation of the unequal quad-band PD circuit is investigated. We denote that Z_{Amin} = min {Z_{A1}, Z_{A2}, Z_{A3}, Z_{A4}}, Z_{Amax} = max {Z_{A1}, Z_{A2}, Z_{A3}, Z_{A4}}; Z_{Bmin} = min {Z_{B1}, Z_{B2}, Z_{B3}, Z_{B3}}, Z_{Bmax} = max {Z_{B1}, Z_{B2}, Z_{B3}, Z_{B4}}. To make the circuit feasible for fabrication, all characteristic impedances in the circuit must be between 15 Ω and 120 Ω. It requires that Z_{Amin}, Z_{Amax}, Z_{Bmin}, and Z_{Bmax} must be in the range from 15 Ω to 120 Ω. Based on equations (14-20) and (6-12), the dependences of impedances Z_{Amin}, Z_{Amax} and Z_{Bmin}, Z_{Bmax} against coefficients $n_1 = f_4/f_1$ and $n_2 = f_3/f_2$ with powers split ratios K^2 of 1.5, 2, 2.5 and 3 are plotted in Figs. 9 and 10.

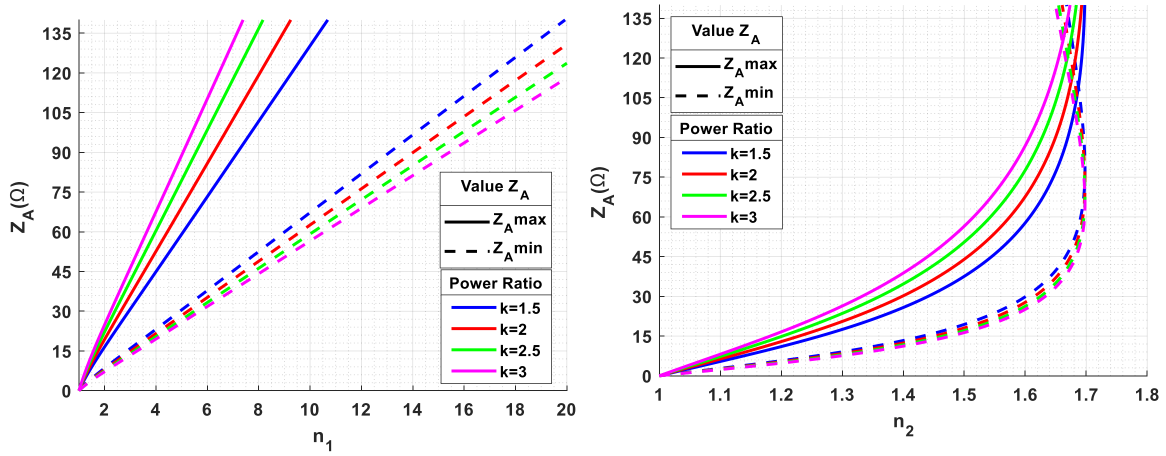

(a) (b)

Fig. 9. (a) The dependence of characteristic impedance Z_{Amin} and Z_{Amax} versus coefficients n_1. (b) The dependence of characteristic impedances Z_{Amin} and Z_{Amax} versus coefficients n_2.

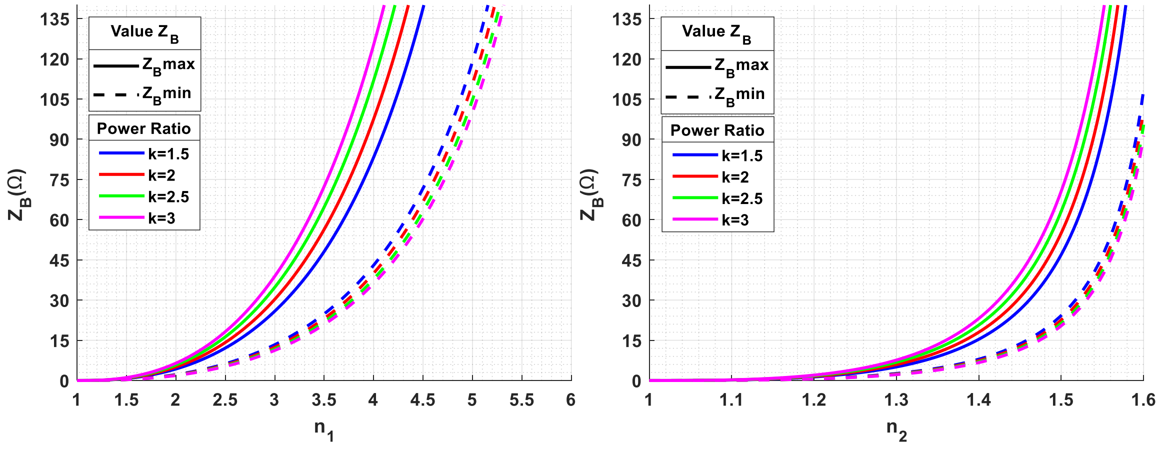

(a) (b)

Fig. 10. (a) The dependence of characteristic impedance Z_{Bmin} and Z_{Bmax} versus coefficients n_1. (b) The dependence of characteristic impedances Z_{Bmin} and Z_{Bmax} versus coefficients n_2.

From Figs. 9 and 10, with given power split ratios, the allowed ranges of frequency ratios n_1 and n_2 can be determined to ensure the manufacturing conditions of the circuit. In particular, with the power split ratio $K^2 = 1.5$, four working frequencies of the circuit must satisfy the following conditions:

$$3.1 \le \frac{f_4}{f_1} \le 4.45, \quad 1.46 \le \frac{f_3}{f2} \le 1.56.$$

Furthermore, based on Figs. 9 and 10, it can be proven that the proposed method for designing unequal quad-band Wilkinson PDs can achieve power split ratios of not more than 2.

4 Fabrication and measurement of quad-band power

To validate the proposed design method, an equal quad-band PD is designed, fabricated, and tested on Rogers RO4003C substrate with a relative dielectric constant of 3.55 and thickness of 0.813 mm.

Applying the design procedure presented in Section 2, parameters of the scheme are calculated. Firstly, we choose frequencies f_4=2.28 GHz and f_1=0.7 GHz. Then, these frequencies are substituted into (12), and electrical length θ_1 is defined as $\theta_1 = 42^{\circ}$. From (8) and (9) the values of Z_K and θ_2 are computed as $Z_K = 83.91\ \Omega$ and $\theta_2 = 72.56^{\circ}$. From (12) the operating frequencies f_2 and f_3 are defined as $f_2 = 1.2$ GHz, $f_3 = 1.78$ GHz. Substituting the values of Z_K and Z_C into (6) and (7) we have $Z_A = 28.36\ \Omega$ and $Z_B = 30.82\ \Omega$. Figure 9 shows the fabricated prototype of the proposed PD. The total area of the PD is 89.2 mm × 75.2 mm.

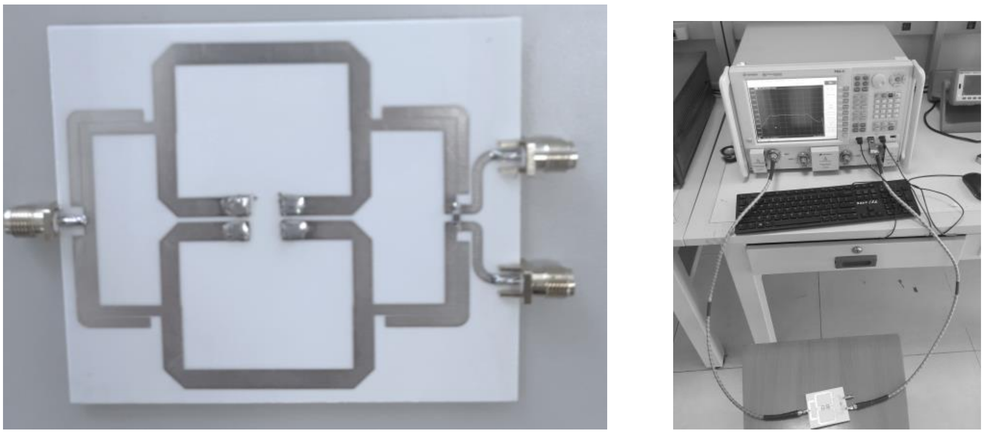

(a) (b)

Fig. 11. Fabricated equal quad-band PD with operating frequencies 0.7 GHz, 1.2 GHz, 1.78 GHz, and 2.28 GHz (a), and experimental setup (b)

The design program Keysight ADS is used for simulation. A Vector Network Analyzer PNA-X N5242A is employed to measure S-parameters of the fabricated quad-band PD (Fig. 11b).

Measurement and simulation results of parameters S_{21} and S_{31} are shown in Fig. 12. The measured results and simulated ones match well with each other. The slight difference between simulation and measurement is mainly caused by SMA connectors which were not de-embedded in the measurement. From Fig. 12 it is clear that measured insertion losses of ports 2 and 3 at four design frequencies are 3.30/3.32 dB, 3.24/3.31 dB, 3.43/3.50 dB and 3.72/3.75 dB, respectively. Therefore, the measured insertion losses of ports 2 and 3 at four central frequencies are consistent with the theoretical values (3 dB) with errors of 0.30/0.32 dB, 0.24/0.31 dB, 0.43/0.5 dB and 0.72/0.75 dB, respectively. These losses are relatively small compared to those of other equal quad-band PDs.

The simulation and measurement of isolation and return losses of the fabricated PD are shown in Fig. 13. It can be seen that the simulation results agree with the measurement ones. Moreover, the isolation level between two output ports is higher than 20.92 dB, and return losses are better than 18 dB at four design bands.

The measured results of AI and PI of the designed circuit are shown in Fig. 14. The amplitude imbalance (AI) and phase imbalance (PI) between the two output ports are determined by expressions

$$AI = |S_{21}\text{-}S_{31}|, \quad PI = |\text{Phase}(S_{21}) - \text{Phase}(S_{31}).|$$

It is clear that amplitude imbalance and phase imbalance are lower than 0.25 dB and 2°, respectively.

Finally, measured performance comparisons between the proposed PD and other published works are shown in Tab. 1.

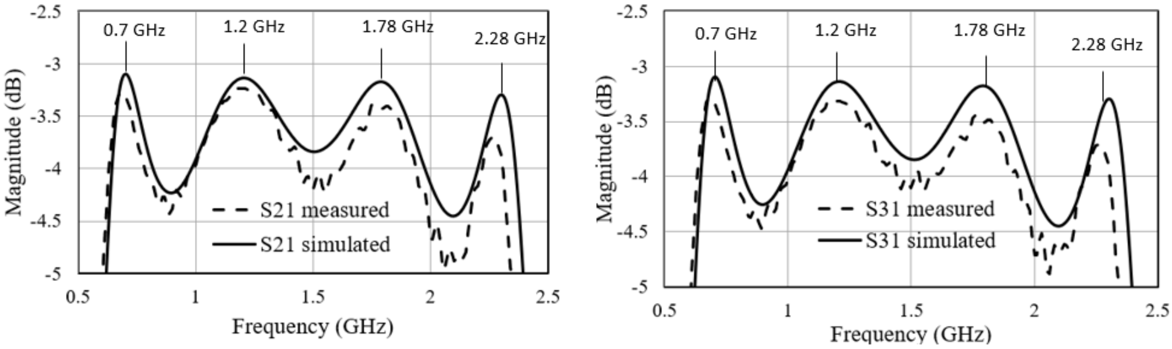

(a) (b)

Fig. 12. Simulation and measurement results of parameters S_{21} (a) and S_{31} (b)

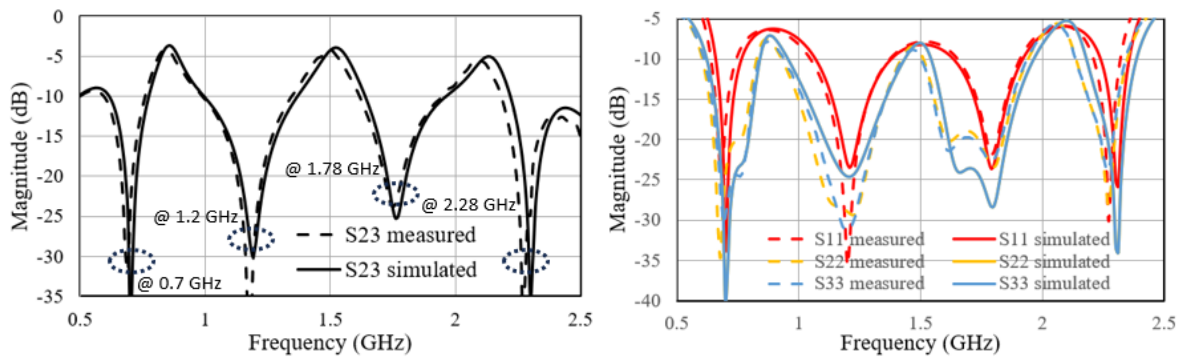

(a) (b)

Fig. 13. Simulation and measurement of S_{23} (a), and S_{11}, S_{22}, S_{33} (b) of the proposed PD

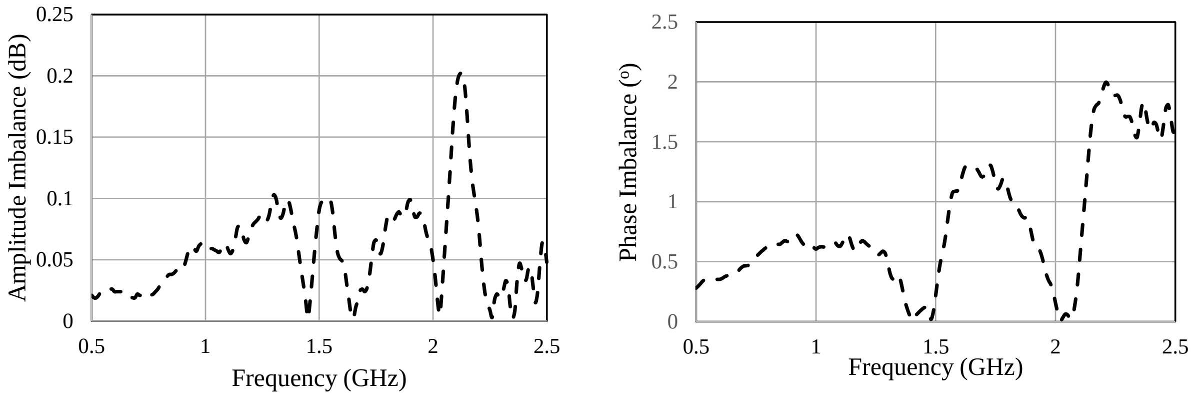

(a) (b)

Fig. 14. Measurement result of the proposed quad-band PD: (a) amplitude imbalance, (b) phase imbalance

Table 1. Comparisons of the measured performances of the proposed equal quad-band PD with other reported equal muti-band PDs

Ref.	Operation	*f* (GHz)	Δ (dB)	IS (dB)	RL (dB)
[20]	Triple-band	3.49/4.13/5.57	< 1.5	> 14.2	> 19
[12]	Triple-band	2.4/3.5/5.2	< 1	> 27	> 42
[14]	Quad-band	1.2/1.66/1.89/2.16	< 1	> 16.3	> 15
[16]	Quad-band	3.34/4.82/6.17/7.66	< 1.85	> 12	> 19
[15]	Quad-band	1.24/ 2.43/3.54/4.63	< 1.75	> 5	> 10
[13]	Quad-band	0.5/1/1.5/2	< 1.5	> 20.7	> 18
[21]	Quad-band	0.898/1.789/2.712/3.581	< 0.95	> 28.6	NI
[17]	Quad-band	2.4/3.5/5.2/5.8	< 1.2	> 18	> 16
[22]	Quad-band	0.5/1.3/2.2/3	< 2	NI	> 19
This work	Quad-band	0.7/1.2/1.78/2.28	< 0.75	> 20.92	>18.14

In Tab. 1, we denote that IS – isolation, RL – return loss, Δ – the largest difference from theoretical values of insertion loss, NI – no information.

It can be seen that the proposed circuit exhibits a low loss compared to previously reported quad-band PDs, while it still ensures good return loss and isolation.

5 Conclusions

In this paper, a simple method to design quad-band PDs is proposed. A quad-band microstrip line is utilized to replace quarter-wavelength transmission line of the conventional Wilkinson PD. Design equations and procedures have been derived for designing the quad-band PDs. Compared with previously reported works, the proposed quad-band PD has the advantage of low insertion loss. Other parameters, such as return loss and isolation reach well. The proposed quad-band PD is prospective for modern microwave systems.

References

[1] K. Song, F. Xia, Y. Zhou, S. Guo and Y. Fan, "Microstrip/Slotline-Coupling Substrate Integrated Waveguide Power Divider with High Output Isolation", *IEEE Microwave and Wireless Components Letters 2019*; 29(2):95 – 7. https://doi: 10.1109/LMWC.2018.2888943.

[2] Bao-Guang Liu, Yun-Peng Lyu, Lei Zhu, Chong-Hu Cheng, "Compact Square Substrate Integrated Waveguide Filtering Power Divider With Wideband Isolation", *IEEE Microwave and Wireless Components Letters 2021*; 31 (2):109-12. https://doi: 10.1109/LMWC.2020.3042332.

[3] Farzad Khajeh-Khalili, Mohammad Amin Honarvar, Ernesto Limiti, "A Novel High-Isolation Resistor-Less Millimeter-Wave Power Divider Based on Metamaterial Structures for 5G Applications", *IEEE Transactions on Components, Packaging and Manufacturing Technology 2021; 11*: 294 – 01. https://doi: 10.1109/TCPMT.2020.3042963.

[4] C. Zhu, J. Zhang, "Design of High-Selectivity Asymmetric Three-Way Equal Wideband Filtering Power Divider 2019", *IEEE Access*; 7: 55329-35. https://doi: 10.1109/ACCESS.2019.2913314.

[5] Yun Liu, Sheng Sun, Lei Zhu, "Design of n-Way Wideband Filtering Power Dividers with Good Port-Port Isolation", *IEEE Transactions on Microwave Theory and Techniques 2021*; 69: 3298-06. https://doi: 10.1109/TMTT.2021.3072365.

[6] Zhenghai Luo, Gang Zhang, Huaiwei Wang, Na Li, Kam Weng Tam, Liming Tang, Wanchun Tang, Jiquan Yang, "Dual-Band and Triple-Band Filtering Power Dividers Using Coupled Lines", *IEEE Transactions on Circuits and Systems II: Express Briefs 2023*; 70(4): 1440-44. https://doi: 10.1109/TCSII.2022.3223922.

[7] S. Ilyas, N. Shoaib, S. Nikolaou and H. M. Cheema, "A Wideband Tunable Power Divider for SWIPT Systems", *IEEE Access 2020*; 8:30675-81. https://doi: 10.1109/ACCESS.2020.2970781.

[8] H. Zhu and Y. J. Guo, "Dual-Band and Tri-Band Balanced-to-Single Ended Power Dividers with Wideband Common-Mode Suppression", *IEEE Transactions on Circuits and Systems II: Express Briefs 2021*; 68: 2332-36. https://doi: 10.1109/TCSII.2021.3054797.

[9] Taegyu Kim, Byungje Lee, and Myun-Joo Park, "Dual-Band Unequal Wilkinson Power Divider with Reduced Length", *Microwave and Optical Technology Letters 2010*; 52: 1187-90. No. 5 May 2010. https://doi:10.1002/mop.25119.

[10] A. Sahu, K. A. Al Shamaileh, P. H. Aaen, S. A. Abu-shamleh and V. K. Devabhaktuni, "A High-Frequency/Power Ratio Wilkinson Power Divider Based on Identical/Non-Identical Multi-T-Sections with Short-Circuited Stubs", *IEEE Open Journal of Circuits and Systems 2021*; 2: 34-45. https://doi: 10.1109/OJCAS.2020.3043354.

[11] K. Al Shamaileh, N. Dib and S. Abushamleh, "A Dual-Band 1:10 Wilkinson Power Divider Based on Multi-T-Section Characterization of High-Impedance Transmission Lines", *IEEE Microwave and Wireless Components Letters 2017*; 27(10): 897-99. https://doi: 10.1109/LMWC.2017.2746665.

[12] Farzad Khajeh-Khalili, M. Amin Honarvar, Abdolmehdi Dadgarpour, Bal S. Virdee, Tayeb A. Denidni, "Compact tri-band Wilkinson power divider based on metamaterial structure for Bluetooth, WiMAX, and WLAN applications", *Journal of Electromagnetic Waves and Applications 2019*; 33 : 707-21. https:// doi: 10.1080/09205071.2019.1575287.

[13] Hussam Jwaied, Firas Muwanes and Nihad Dib, "Design and analysis of quad-band Wilkinson power divider", *International Journal on Wireless and Optical 2007*; 7: 305-12. https:// doi:10.1142/S0219799507000680.

[14] Zhengyu Sun, Gang Zhang, Xinyu Yang, Liming Tang, "A miniature microstrip quad-band filtering power divider based on quad-mode resonators". *IET Microwaves, Antennas & Propagation 2022*; 16: 950-54. https://doi.org/10.1049/mia2. 12293.

[15] R. Gómez-García, R. Loeches-Sánchez, D. Psychogiou and D. Peroulis, "Single/multi-band Wilkinson-type power dividers with embedded transversal filtering sections and application to channelized filters*", IEEE Transactions on Circuits and Systems I: Regular Papers 2015*; 62: 1518-27. https://doi: 10.1109/TCSI.2015.2418838.

[16] N. C. Pradhan, K. S. Subramanian, R. K. Barik and Q. S. Cheng, "Design of Compact Substrate Integrated Waveguide Based Triple- and Quad-Band Power Dividers", *IEEE Microwave and Wireless Components Letters 2021*;31:365-68. https://doi: 10.1109/LMWC.2021.3061693.

[17] Hemn Younesiraad, Mohammad Bemani, Mahdi Fozi, "A novel fully planar quad band Wilkinson power divider", *AEU - International Journal of Electronics and Communications 2017*; 74: 75-2. https://doi.org/10.1016/j.aeue.2017.01.020.

[18] D. M. Pozar, *Microwave engineering*, 4th ed. New York: Wiley; 2012.

[19] A. A. Althuwayb, "Design of quad-band rat-race coupler for GSM/WiMAX/WLAN/Satellite Applications", *Radioengineering 2021*; 30: 135-41. https://doi: 10.13164/re.2021.0135.

[20] K. Song, M. Fan, F. Zhang, Y. Zhu and Y. Fan, "Compact Triple-Band Power Divider Integrated Bandpass-Filtering Response Using Short-Circuited SIRs", *IEEE Trans-actions on Components, Packaging and Manufacturing Technology 2017*; 7:1144-50. https://doi:10.1109/TCPMT.2017.2687468.

[21] Bin Xia, Lin-Sheng Wu, Junfa Mao & Lin Yang, "A new quad-band Wilkinson power divider", *Journal of Electromagnetic Waves and Applications 2014*;28: 1622-34. https://doi: 10.1080/09205071.2014.938170.

[22] H. H. Jaradat, N. I. Dib and K. A. Al Shamaileh, "A Compact Coplanar Waveguide Quad-Band Wilkinson Power Divider Using Non-Uniform Transmission Lines", *International Applied Computational Electromagnetics Society Symposium (ACES) 2019*: 1-2.

Received 4 December 2023